6

Donor-Acceptor Conjugated Polymers and Their Nanocomposites for Photonic Applications

D. Udaya Kumar[1], A. John Kiran[2], M. G. Murali[1] and A. V. Adhikari[1]
[1]*Department of Chemistry, National Institute of Technology Karnataka, Surathkal, P. O. Srinivasnagar,*
[2]*Department of Inorganic and Physical Chemistry, Indian Institute of Science, Bangalore*
India

1. Introduction

Organic materials exhibiting strong nonlinear optical (NLO) properties have attracted considerable interest in recent years because of their promising applications in opto-electronic and all-optical devices such as optical limiters, optical switches and optical modulators (Munn & Ironside, 1993; Zyss, 1994). A variety of organic materials, including conjugated molecules, polymers and dyes, have been investigated for their NLO responses (Kamanina, 1999, 2001; Kamania & Plekhanov, 2002; Kamanina et al., 2008, 2009). Conjugated organic polymers have emerged as a promising class of NLO materials because of their large nonlinear responses associated with fast response time, in addition to their structural variety, processability, high mechanical strength, and excellent environmental and thermal stability (Prasad & Williams, 1992). In contrast to misconceptions about the frailty of simple organic molecules, the optical damage threshold for polymeric materials can be greater than 10 GW/cm^2. Among various π-conjugated materials, thiophene based polymers are currently under intensive investigation as materials for nonlinear optics because of their large third-order nonlinear response, chemical stability and their readiness of functionalization (Kishino et al., 1998; Nisoli et al, 1993; Sutherland, 1996, Udayakumar et al., 2006).

It has been well-known that, the strong delocalization of π-electrons along the backbone of conjugated polymers determines very high molecular polarizability and thus causes remarkable optical nonlinearities. However, a necessary step in further improving the NLO properties of conjugated polymers is to understand the fundamental relationship that exists between the molecular structure and the hyperpolarizabilities. A deeper understanding in this subject will improve the design of organic conjugated molecules and polymers by a judicious choice of functional substituents to tune their optical properties for photonic applications. Cassano et al. had reported a strategy for tuning the linear and nonlinear optical properties of soluble poly(paraphenylenevinylene) derivatives, based on the effect of simultaneous presence of electron-acceptor and electron-donor units in the conjugated backbone (Cassano, 2002). Particularly, they reported that the value of third-order nonlinear susceptibility ($\chi^{(3)}$) obtained for the

polymer containing alternating phenylenevinylene and tetrafluorophenylenevinylene units was one order of magnitude larger than that measured for the corresponding homopolymer, poly(paraphenylenevinylene) (PPV). Similarly, Chen et al. reported the third-order optical nonlinearity of a conjugated 3,3′ - bipyridine derivative, with an enhanced nonlinearity due to its symmetrical donor-acceptor-donor structure, in which the 3,3′ - bipyridine core was acting as the acceptor group and the thiophene ring as the donor group (Chen, 2003). The donor-acceptor (D-A) approach, introduced by Havinga et al. (1993) in macromolecular systems via alternating electron-rich and electron-deficient substituents along the conjugated backbone, has attracted a good deal of attention in recent years. Interaction of the donor–acceptor moieties enhances the double bond character between the repeating units, which stabilizes the low band gap quinonoid like forms within the polymer backbones. Hence, a conjugated polymer with an alternating sequence of the appropriate donor and acceptor units in the main chain can induce a reduction in its band gap energy. Recently, molecular orbital calculations have shown that the hybridization of the energy levels of the donor and the acceptor moieties result in D-A systems with unusually low HOMO-LUMO separation (Brocks & Tol, 1996). If the HOMO levels of the donor and the LUMO levels of the acceptor moiety are close in energy, the resulting band structure will show a low energy gap. Further reduction in band gap is possible by enhancing the strength of donor and acceptor moieties via strong orbital interactions. In addition, the presence of strong electron donors and acceptors in conjugated polymers increases the π-electron delocalization leading to a high molecular polarizability and thus improving the nonlinear response of the polymer. In this direction, several donor-acceptor type conjugated polymers were synthesized and their third-order nonlinear optical properties were investigated (Hegde et al., 2009; Kiran et al., 2006, Udayakumar et al., 2006, 2007).

Metal and semiconductor nanoparticles are also emerging as a promising class of NLO materials for nanophotonic applications (Fatti & Vallee, 2001; Gayvoronsky et al., 2005; Philip et. al., 2000; Venkatram et. al., 2005; Voisin et al., 2001). For instance, a large nonlinear optical response with a third-order NLO susceptibility ($\chi^{(3)}$) value as high as 2×10^{-5} esu has been observed for nanoporous layers of TiO_2 (Gayvoronsky et al., 2005). Research has shown that it is advantageous to embed metal/semiconductor nanoparticles in thin polymer films for application purposes because the polymer matrix serves as a medium to assemble the nanoparticles and stabilize them against aggregation (Boyd, 1996; Takele et al., 2006). Furthermore, the nanocomposite structures are known to substantially enhance the optical nonlinearities (Neeves & Birnboim 1988). Therefore, the third-order NLO properties of several metal/semiconductor-polymer nanocomposites have been investigated (Gao et al., 2008; Karthikeyan et al., 2006; Porel et al., 2007). Recently, conjugated polymers are being used as host matrix for dispersing metal/semiconductor nanoparticles (Sezer et al., 2009). Such nanoparticle/polymer composites are shown to possess a large third-order nonlinear susceptibility of the order of 10^{-7} esu with an ultrafast response time of 1.2 ps (Hu et al., 2008). The nanocomposites made of Ag nanoparticles dispersed in poly[2-methoxy-5-(2-ethylhexyloxy)-1,4-phenylenevinylene] matrix have exhibited a large third-order nonlinear susceptibility of the order of 10^{-6} esu (Hu et al., 2009). Higher $\chi^{(3)}$ value has been observed for polydiacetylene-Ag nanocomposite film when compared with the pure polydiacetylene film (Chen et al., 2010).

In this chapter, we describe the third-order nonlinear optical studies on new donor-acceptor conjugated polymers; named as PThOxad 1a-c, PThOxad 2a-c and PThOxad 3a-c. All these

polymers contain 3,4-diakoxythiophene units as electron donors and 1,3,4-oxadiazole as electron acceptor units. Nanocmposites of PThOxad 3c and nano TiO_2 were prepared using the spin coating method. The third-order nonlinear optical properties of the polymers and their composites were investigated using z-scan and degenerate four wave mixing (DFWM) techniques. All the polymers exhibit significant third-order nonlinearity. We describe their concentration dependent optical limiting behavior using a ns Nd:YAG laser operated at 532 nm.

2. Experimental set up

Z-scan (Bahae et al., 1990) is a technique that is particularly useful when nonlinear refraction is accompanied by nonlinear absorption. This method allows the simultaneous measurement of both the nonlinear refractive index and the nonlinear absorption coefficient of a material. Basically, the method consists of translating a sample through the focus of a Gaussian beam and monitoring the changes in the far-field intensity pattern. Because of the light-induced lens-like effect, the sample has a tendency to recollimate or defocus the incident beam, depending on its z position with respect to the focal plane. By properly monitoring the transmittance change through a small aperture placed at the far-field position (closed aperture), one is able to determine the amplitude of the phase shift. By moving the sample through the focus and without placing an aperture at the detector (open aperture), one can measure the intensity-dependent absorption as a change of transmittance through the sample.

A Q-switched Nd:YAG laser with a pulse width of 7 ns at 532 nm was used as a source of light in the z-scan experiment. The output of the laser had a nearly Gaussian intensity profile. A lens of focal length 26 cm was used to focus the laser pulses onto the sample. The resulting beam waist radius at the focused spot, calculated using the formula $w_0 = 1.22\lambda f / d$, where f is focal length of the lens and d is the diameter of the aperture, was found to be 20 μm. The corresponding Rayleigh length, calculated using the formula, $z_0 = \pi w_0^2 / \lambda$ was found to be 2.3 mm. Thus the sample thickness of 1 mm was less than the Rayleigh length and hence it could be treated as a thin medium. The scan was obtained with a 50% (S = 0.5) aperture and at pulse energy of 10 μJ, which corresponds to a peak irradiance of 0.22 GW/cm^2. In order to avoid cumulative thermal effects, data were collected in single shot mode (Yang, 2002). The optical limiting measurements were carried out when the sample was at focal point by varying the input energy and recording the output energy. Both the incident and the transmitted energies were measured simultaneously by two pyroelectric detectors with Laser Probe Rj-7620 Energy Ratio meter. Spectral grade dimethylformamide (DMF) was used for the preparation of polymer solutions.

Four-wave mixing refers to the interaction of four waves in a nonlinear medium via the third-order polarization. When all the waves have same frequency, it is called as degenerate four-wave mixing. There are several geometries used in studying this phenomenon. One of such geometries used in our experiment is the backward geometry or the phase conjugate geometry. Here, two counter propagating strong beams are called forward pump beam and the backward pump beam. A third wave called the probe beam is incident at small angle θ (~ 4^o) to the direction of the forward pump. A fourth beam, called the conjugate beam, is generated in the process and propagates counter to the probe beam (Sutherland, 1996). In the

present study, the laser energy (at 532 nm) at the sample was varied by the combinations of neutral density filters. Sample was taken in a 1 mm thick glass cuvette, with a concentration of 10^{-5} mol/L. A small portion of the pump beams was picked off and measured by a photodiode to monitor the input energy. The DFWM signal generated in the sample solution was separated by a second photodiode. The photodiode signals were averaged over a number of laser shots and displayed by a Tektronix TDS2002 digital storage oscilloscope.

3. Polymers and their nanocomposites

Introduction of strong electron donor and strong electron acceptor groups along polymer chain could be a promising molecular design to improve the NLO properties in D-A type polymers. Processing of these polymers for application purposes requires good solubility in common organic solvents. Another important criterion from the application point of view is the good film forming properties of these polymers. Solubility of the polymers could be improved by the incorporation of proper solubilising groups either in the polymer main chain or in the side chain. Keeping these points in view, three series of D-A polymers (PThOxad 1a-c, PThOxad 2a-c and PThOxad 3a-c) are synthesized in the present study and are characterized. The polymer structures consist of electron donating 3,4-dialkoxythiophene units and electron accepting 1,3,4-oxadiazole units. In 3,4-dialkoxythiophnes, introduction of long alkoxy pendants at 3– and 4– positions of the thiophene ring not only enhances the electron donating nature of the ring but also improves the solvent processability of the corresponding polymer. On the other hand, 1,3,4-oxadiazole ring, due to its high electron affinity, is a good electron acceptor for D-A type conjugated polymers. However, in the case of poly(3,4-dialkoxythiophene)s the steric interactions of alkoxy groups of adjacent thiophene rings reduce the coplanarity and hence it affects the conjugation length of the polymer. In order to minimize such steric interactions two strategies have been employed in the present study. First one is to introduce a spacer unit, like a 1,4-divinylbenzene moiety as is the case in PThOxad 1a-c (Fig. 1) or a phenyl ring (PThOxad 3a-c), along the polymeric backbone so that the thiophene rings are well separated, which thus minimizes the steric interactions of the alkoxy groups. Second method is to replace one of the 3,4-dialkoxythiophene units by a cyclosubstituent fused at 3– and 4–positions, i.e. 3,4-ethylenedioxythiophene (EDOT) unit (PThOxad 2a-c), so that there will not be any steric interactions. These polymers are synthesized by using a precursor polyhydrazide route. As expected, all these polymers showed good solubility in common organic solvents, which is an important requirement for the processing of the polymers for device applications.

The chemical structures of the D-A polymers containing 3,4-dialkoxythiophenes and 1,3,4-oxadiazole units are shown in Fig. 2. The synthetic route for these polymers involves the preparation of monomer units, which follows the polycondensation of these monomeric units to give the final polymers. As a representative, the synthesis of PThOxad 1a-c is described in this section. A series of monomers, 3,4-dialkoxythiophene-2,5-carbonyldihydrazides (6a-c) were prepared starting from thiodiglycolic acid (1). Esterification reaction of thiodiglycolic acid (1) with ethanol in presence of conc.sulphuric acid afforded diethylthiodiglycolate (2). Compound 2 was then condensed with diethyloxalate in presence of sodium ethoxide and ethanol to get diethyl 3,4-dihydroxythiophene-2,5-dicarboxylate disodium salt (3). Acidification of the disodium salt with hydrochloric acid afforded the compound 4.

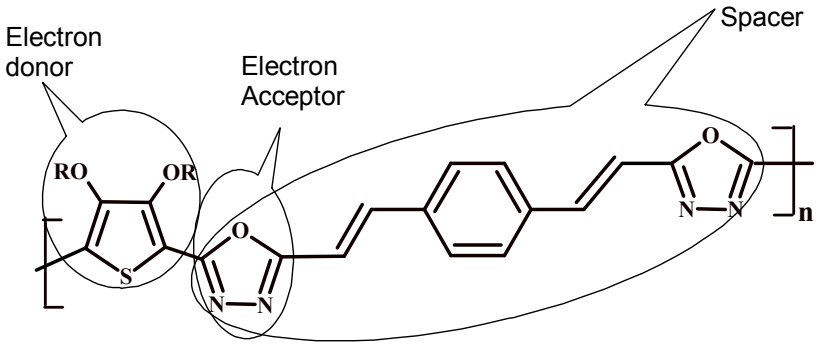

Fig. 1. Chemical structures of donor-acceptor conjugated polymers, PThOxd 1a-c, showing donor, acceptor and spacer units.

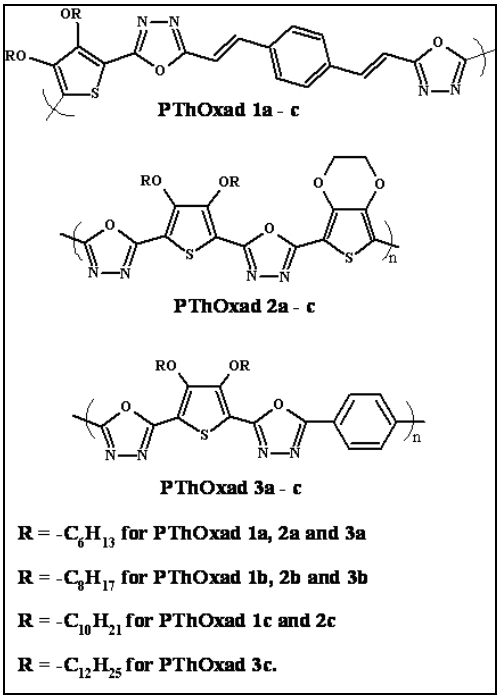

Fig. 2. General structures of the polymers, PThOxad 1a-c, PThOxad 2a-c and PThOxad 3a-c.

Diethyl 3,4-dialkoxythiophene-2,5-dicarboxylates (5a-c) were synthesized by the etherification reaction of diethyl 3,4-dihydroxythiophene-2,5-dicarboxylate (4) with the corresponding n-bromoalkane in the presence of potassium carbonate and DMF. The reaction was completed in 70 h. Diethyl 3,4-dialkoxythiophene-2,5-dicarboxylates (5a-c) were then converted into corresponding 3,4-dialkoxythiophene-2,5-carbonyldihydrazides (6a-c) by treating them with hydrazine hydrate and methanol. Scheme 2 shows synthetic

route to the synthesis of 3,3′-(1,4-phenylene)bis[2-propenoyl chloride] (8), which was achieved starting from 1,4-benzenedicarboxaldehyde. Knoevenagel condensation of 1,4-benzenedicarboxaldehyde (7) with malonic acid in presence of pyridine and a catalytic amount of piperidine afforded 3,3′-(1,4-phenylene)bis[2-propenoic acid], which on treatment with thionyl chloride utilizing DMF as a catalyst yielded the monomer 8. The chemical structures of all the above compounds were confirmed by spectral and elemental analyses.

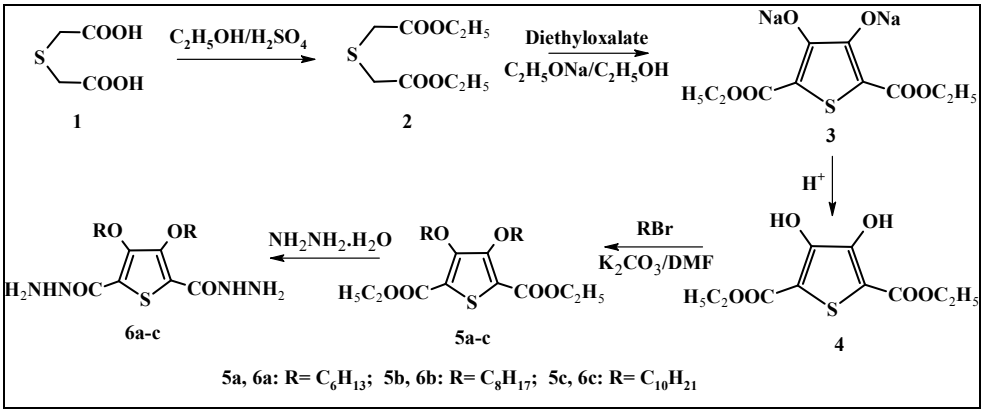

Scheme 1. Synthesis of 3,4-dialkoxythiophene-2,5-carbonyldihydrazides (6a-c).

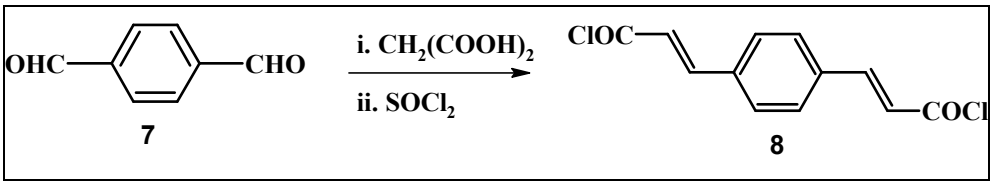

Scheme 2. Synthesis of 3,3′-(1,4-phenylene)bis[2-propenoyl chloride] (8)

The synthetic route for PThOxad 1a-c is involves the synthesis of precursor polyhydrazides followed by the conversion these polyhydrazides into polyoxadiazoles (scheme 3). For the preparation of polyhydrazides, a mixture of 10 mmol of appropriate dihydrazide, 20 mmol of anhydrous lithium chloride and 0.1 ml of pyridine was taken in 20 ml of N-methylpyrrolidinone, and 10 mmol of acid chloride (8) was added slowly at room temperature under N_2 atmosphere. The reaction mixture was stirred at room temperature for 5 h. The resultant yellow solution was heated at 80 ^oC with stirring for 20 h. After cooling to room temperature the reaction mixture was poured into water to get a precipitate. The precipitate was collected by filtration and was washed thoroughly with water followed by acetone and finally dried in vacuum to get the corresponding polyhydrazides in 70-85% yield. These polyhydrazides are insoluble in common organic solvents at ambient and even at elevated temperatures, as reported for other polyhydrazides. The polyhydrazides were converted into the corresponding poly(1,3,4-oxadiazole)s, by cyclodehydration of the

hydrazide group into 1,3,4-oxadiazole ring, using polyphosphoric acid (PPA), which functions both as solvent and dehydrating agent. The reaction was carried out by heating a mixture of polyhydrazide (0.5 g) and 50 ml of polyphosphoric acid at 100 °C for 4 h under N_2 atmosphere. The reaction mixture was then cooled to room temperature and poured into excess of water. The resulting precipitate was collected by filtration, washed thoroughly with water followed by acetone and dried in oven at 70 °C to get the final polymers in 70 - 80% yield. The progress of the cyclodehydration reaction was monitored by FTIR spectroscopy. The stretching bands of C = O and N – H groups of polyhydrazides (fig.3), disappeared in the FTIR spectra of the corresponding poly(oxadiazole)s, where as the band corresponding to imine (C = N) in an oxadiazole ring was newly generated (fig. 4). In addition, peaks due to =C–O–C= (1,3,4-oxadiazole ring) stretching was also observed for these polymers, confirming the conversion of polyhydrazides to polyoxadiazoles.

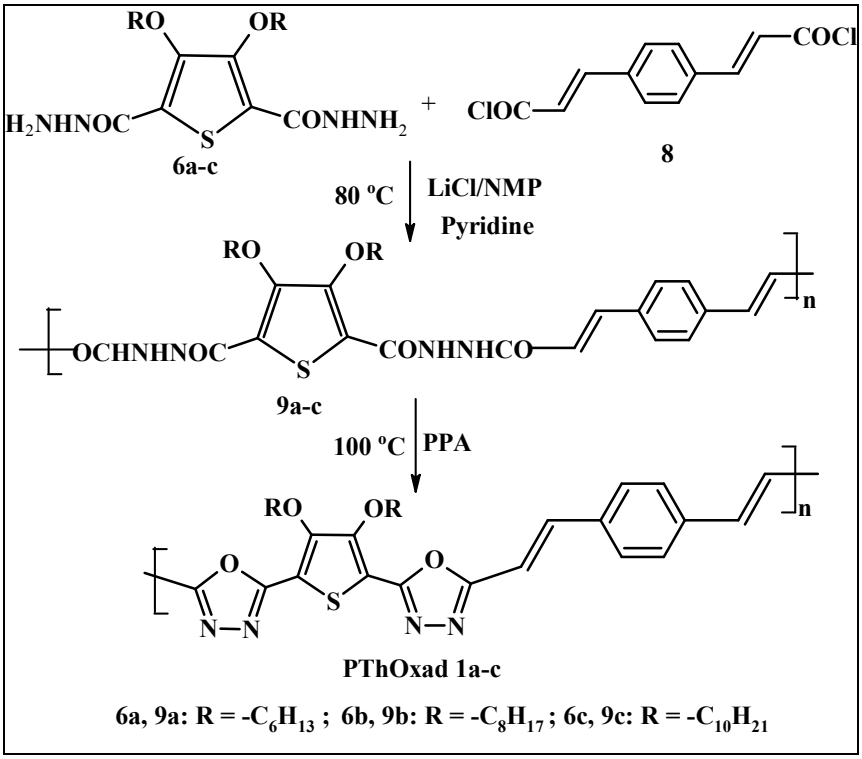

Scheme 3. Synthesis of polymers, PThOxad 1a-c.

The polymers are found to be thermally stable up to ~330 ◦C. DSC studies were performed to observe glass transition temperature (T_g) of the polymers. The samples were heated up to 300 ◦C under nitrogen atmosphere at a heating rate of 5 ◦C/min. No T_g or melting point was observed suggesting that the polymers are either having very high T_g or are highly crystalline in nature and decompose before melting.

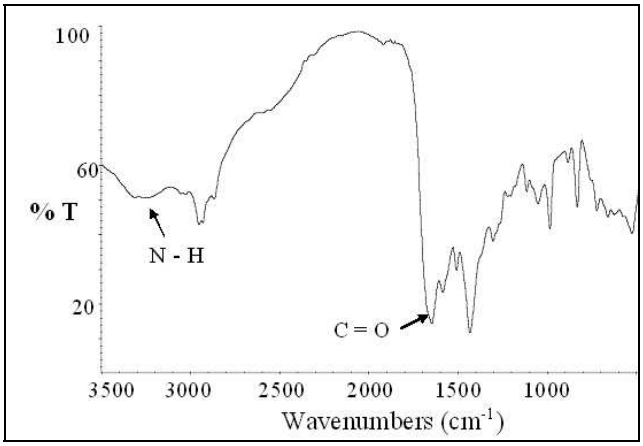

Fig. 3. FT-IR sprectrum of polyhydrazide 9c.

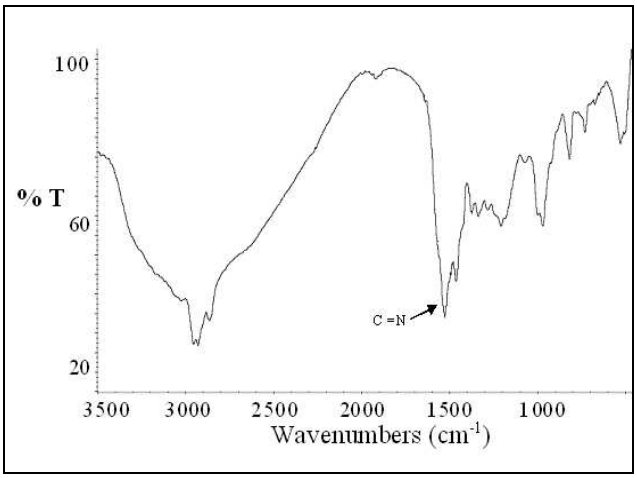

Fig. 4. FT-IR sprectrum of polyoxadiazole, PThOxad 1c.

The UV–vis absorption and fluorescence spectra of the polymers (PThOxad 1a-c) were recorded both in solution and in thin film form. As shown in fig. 5, the absorption maxima of the polymers in dilute DMF solutions (ca. 10^{-5}) are 373 nm for PThOxad 1a, 378 nm for PThOxad 1b and 381 nm for PThOxad 1c. In addition, the absorption spectra of the polymers displayed a shoulder at 306 nm. Compared with poly(3,4-dialkoxythiophenes), these polymers showed a red shift in absorption spectra. This may be due to the presence of 1,4- divinylbenzene moiety in PThOxad 1a-c, which serves to alleviate steric effects of the alkoxy groups in the adjacent thienylene rings. Hence, electron-donating contributions from the alkoxy groups to the electronic structure of the polymers become more prominent. The absorption spectra of the polymer thin films (fig. 6) are rather broad and so their λ_{max} values could not be precisely determined. However, their optical energy band gap (E_g) was calculated from the absorption edge in the thin films to be 2.20–2.38 eV. As shown in fig. 7,

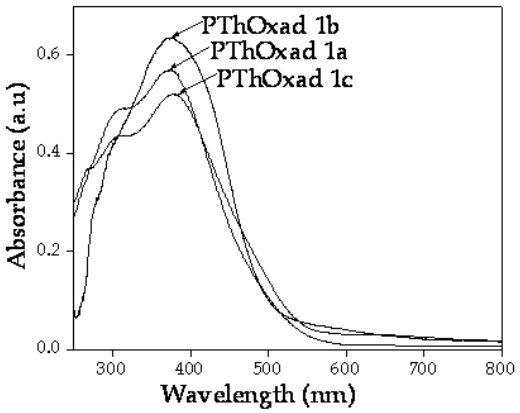

Fig. 5. UV-visible absorption spectra of PThOxad 1a-c in DMF solution.

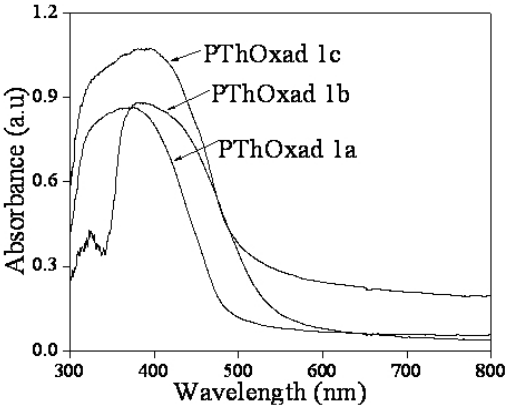

Fig. 6. UV-visible absorption spectra of PThOxad 1a-c as thin films.

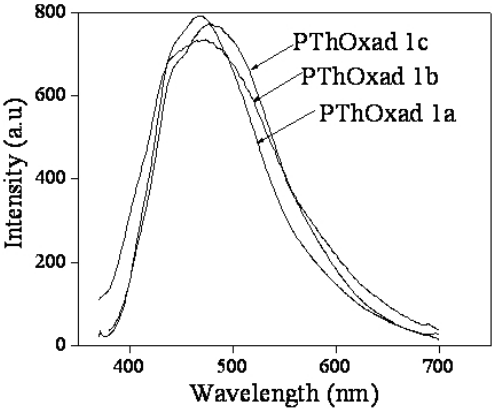

Fig. 7. Fluorescence emission spectra for PThOxad 1a-c in DMF solution.

the emissive maxima of the polymers in dilute DMF solutions (ca. 10^{-5}) are 470 nm for PThOxad 1a, 474 nm for PThOxad 1b, and 479 nm for PThOxad 1c. The Stokes shift was determined to be 97, 96 and 98 nm for PThOxad 1a-c, respectively. The fluorescence emission spectra of these polymers in thin films are shown in fig. 8. The polymers emit intense green light in solid state, with emission peaks at 502, 506 and 512 nm for PThOxad 1a-c, respectively. Consequently, the fluorescence spectra of the polymer thin films exhibit a red shift with respect to those obtained from their solutions. This can be attributed to the interchain or/and intrachain mobility of the excitons and excimers generated in the polymer in the solid stated phase. Further, a sequential red shift in the λ_{max} was observed in both the UV–vis absorption spectra and fluorescence emission spectra of polymers. The increase in the length of the alkoxy side chains led to a red shift in the λ_{max} in UV–vis absorption and fluorescence emission spectra. This can be interpreted as an expected better side chain interdigitation and interchain organization with increasing pendant chain length. The fluorescence quantum yields (Davey et al., 1995) of the polymers in solution were determined using quinine sulfate as a standard (Demas & Grosby, 1971) and are found to be in the range of 26–30%. Following the similar procedure for PThOxad 1a-c, other two series of polymers, PThOxad 2a-c and PThOxad 3a-c, were prepared and their optical properties were studied.

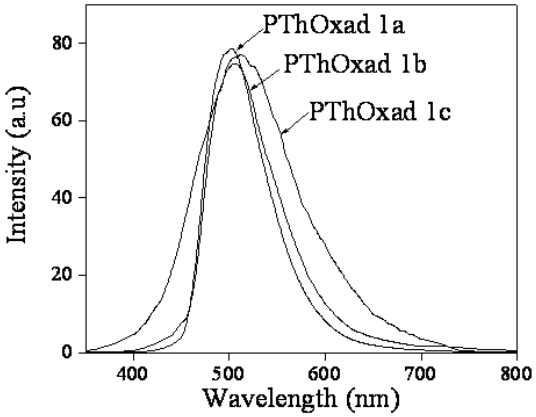

Fig. 8. Fluorescence emission spectra for PThOxad 1a-c as thin films.

For the preparation of PThOxad 3c/TiO_2 nanocomposite, polymer (PThOxad 3c) and TiO_2 were dispersed in the weight ratio 4:1 in chloroform and chlorobenzene solvent system (10:1 volume ratio) and sonicated for 2 hrs. Nanocomposite films were prepared on clean glass plates through spin coating and the films were dried in vacuum for 1 hr. The thickness of the polymer and the nanocomposite films was determined by the SEM cross section, and was found to be in the range of 0.5 – 1 micrometer. The linear transmittance of the film samples was between 50 to 60 % aqt 532 nm. The thermogravimetric analysis (TGA) of PThOxad 3c and PThOxad 3c/TiO_2 nanocomposite was carried out under nitrogen atmosphere at a heating rate of 5 ^oC/min. The polymer (PThOxad 3c) decomposed slowly in the temperature region of 190 – 310 ^oC and thereafter a rapid degradation took place up to 495 ^oC. The nanocomposite started to decompose at 300 ^oC (fig. 9) which indicated a higher thermal stability of the nanocomposite in comparison with that of the polymer. A similar

thermal stabilization of nanocomposite was reported in the literature (Zhu et al., 2008). Fig.10 shows the SEM image of the PThOxad 3c/TiO_2 nanocomposite. A moderately uniform distribution of TiO_2 nanoparticles can be observed with average particle sizes ranging from 25 to 45 nm.

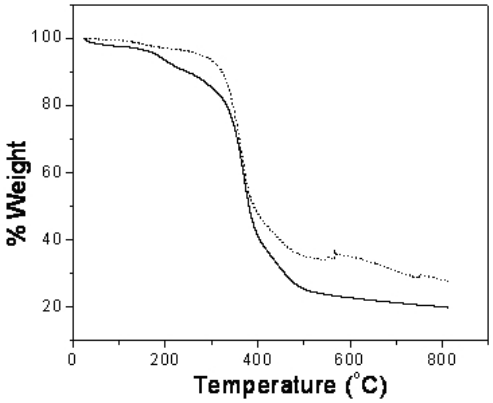

Fig. 9. TGA graphs for PThOxad 3c (—) and PThOxad 3c/TiO_2 nanocomposite (---).

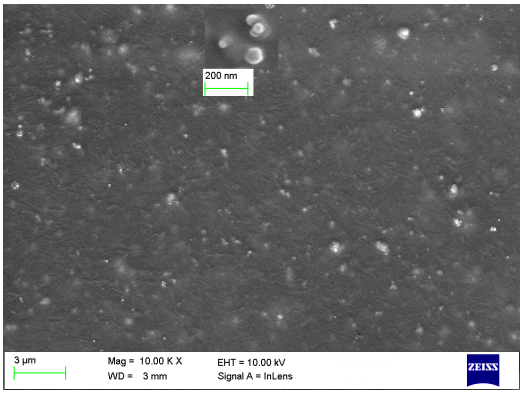

Fig. 10. SEM images of PThOxad 3c/TiO_2 nanocomposite (Inset: magnified image, Mag. = 100 K X).

The UV-vis absorption spectra of PThOxad 3c in $CHCl_3$ solution (ca.10^{-5}), PThOxad 3c film and PThOxad 3c/TiO_2 nanocomposite film are shown in fig. 11. PThOxad 3c in solution displayed an absorption maximum at 378 nm, while the PThOxad 3c film showed a red shift of 16 nm in the absorption spectrum. The optical energy band gap (E_g) of PThOxad 3c was calculated from the absorption edge in the film and was found to be 2.28 eV. The PThOxad 3c/TiO_2 nanocomposite film showed an absorption peak at 412 nm ($\pi \rightarrow \pi^*$ of polymer) and at 310 nm and a shoulder at 250 nm (characteristic absorptions of TiO_2). Fig. 12 shows the fluorescence emission spectra for PThOxad 3c in $CHCl_3$ solution (ca.10^{-4} g/l), PThOxad 3c film and PThOxad 3c/TiO_2 nanocomposite film. Incorporation of TiO_2 nanoparticles caused

a slight red shift in the absorption spectra and a blue shift in the emission spectra. There was a shift of 18 nm in the absorption maximum of the nanocomposite film, when compared with that of the polymer film. We note that, a similar red shift in the absorption maximum was reported for MEH-PPV/TiO_2 nanocomposite films (Yang et al., 2007). A blue shift of 26 nm was observed in the emission maximum of PThOxad 3c/TiO_2 nanocomposite film in comparison with that of the polymer film. Although the exact reasons for these shifts are not well understood, these optical results indicate that some interactions can occur between the conjugated polymer chains and TiO_2 nanoparticles. It can be suggested that these interactions will modify the polaronic states of the polymer and increase the excitonic energy. Therefore, the emission spectrum of PThOxad 3c/TiO_2 nanocomposite will shift toward higher photo energies than those of the PThOxad 3c resulting in a blue shift in the emission spectrum (Hsieh et al., 2007).

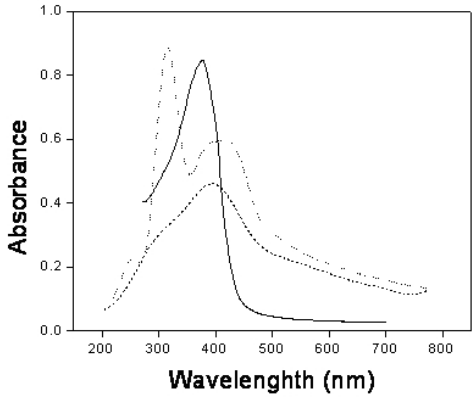

Fig. 11. UV-vis absorption spectra for polymer solution in chloroform (—), polymer film (---) and nanocomposite film (…).

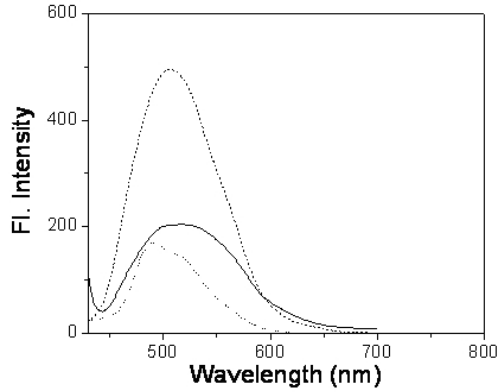

Fig. 12. Fluorescence emission specta of the polymer solution in chloroform (---), polymer film (—) and nanocomposite film (…).

4. Results and discussion

4.1 Polythiophenes

Fig. 13 shows the open aperture z-scan results obtained at 532 nm for PThOxad 1a-c samples dissolved in DMF. The transmission is symmetric about the focus (z = 0) where it has a minimum transmission. Thus an intensity dependent absorption effect is observed. The solid line in Fig. 13 is a fit of data to equation (1), by assuming only two-photon absorption (2PA). The normalized transmission for the open aperture condition (Henari et al., 1997) is given by,

$$T(z) = 1 - \frac{q_0}{2\sqrt{2}} \quad \text{for } q_0 < 1, \tag{1}$$

where:

$$q_0(z) = \frac{\beta I (1 - \exp^{-\alpha L})}{(1 + z^2/z_0^2)\,\alpha}.$$

Here, β is the nonlinear absorption coefficient, L is the length of the sample, I is the intensity of the laser beam at the focus, z is the position of the sample and z_0 is the Rayleigh range of the lens. A fit of open aperture data with equation (1) yields the value of β in the range of 50 to 80 cm/GW for the polymer samples. We note that, the linear absorption spectra of PThOxad 1a-c (fig. 5) show that the polymers are not fully transparent at 532 nm; the linear absorption coefficients (α) for polymers at 532 nm are tabulated in Table 1. Therefore, there can be various mechanisms, such as the excited state absorption (ESA), that are responsible for such a large nonlinear absorption in these polymers.

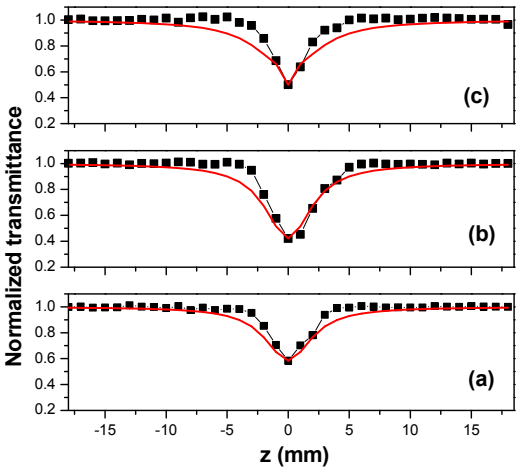

Fig. 13. Open aperture curves for PThOxad 1a (a), PThOxad 1b (b) and PThOxad 1c (c). Solid line is a fit of data to equation (1) assuming only 2PA, with β =73.8 cm/GW for PThOxad 1a, β = 53 cm/GW for PThOxad 1b and β =63.6 cm/GW for PThOxad 1c.

Fig. 14 represents different nonlinear absorption (NLA) mechanisms using an energy level diagram. The diagram shows the different energy levels of a molecule, the singlet ground state S_0, the excited singlet states S_1 and S_2, as well as the triplet excited states T_1 and T_2. It also displays the different transitions taking place between these energy levels. When two photons, of the same or different energy are simultaneously absorbed from the ground state to a higher excited state ($S_0 \rightarrow S_1$), it is denoted as two-photon absorption (2PA). When the excited state absorption (ESA) occurs, molecules are excited from an already excited state to a higher excited state (e.g. $S_1 \rightarrow S_2$ and/or $T_1 \rightarrow T_2$). For this to happen the population of the excited states (S_1 and/or T_1) needs to be high so that the probability of photon absorption from that state is high. The ESA could be enhanced if the molecules could undergo intersystem crossing (ISC) to the triplet state. If more absorption occurs from the excited state than from the ground state it is usually called as the reversed saturable absorption (RSA). The triplet excited state absorption may result in RSA if the absorption cross section of triplet excited state is greater than that of singlet excited state. With excitation of laser pulses on the nanosecond scale, triplet-triplet transitions may make a significant contribution. Nevertheless, such an increased nonlinear absorption due to additional excited state absorption will result in a strong optical limiting activity of the material.

The excited state cross section (σ_{ex}) can be measured from the normalized open aperture z-scan data (Henari et al., 1997). It is assumed that the molecular energy levels can be reduced to a three level system in order to calculate σ_{ex}. Molecules are optically excited from the ground state to the singlet-excited state and from this state they relax either to the ground state or the triplet state, when excited state absorption can occur from the triplet to the higher triplet excited state.

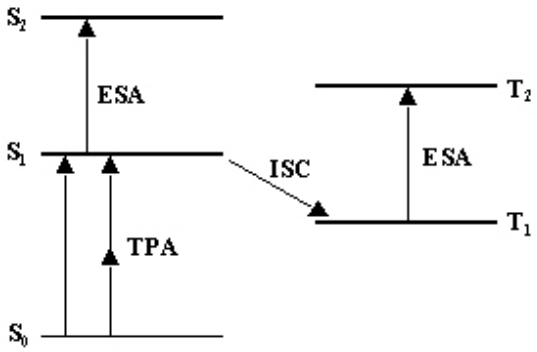

Fig. 14. Energy level diagram showing both two-photon absorption and excited state absorption.

The change in the intensity of the beam as it passes through the material is given by,

$$\frac{dI}{dz} = -\alpha I - \sigma_{ex} N(t) I \,,$$

where I is the intensity and N is the number of molecules in the excited state. The excited state density of molecules appears as a result of a nonlinear absorption process, whose intensity dependence can be obtained from,

$$\frac{dn}{dz} = \frac{\sigma_{ex} I}{h\nu},$$

where ν is the frequency of the laser. Combining the above two equations and solving for the fluence of the laser and integrating over the spatial extent of the beam gives the normalized transmission for open aperture as

$$T = \ln\left(1 + \frac{q_0}{1+x^2}\right) / \frac{q_0}{1+x^2} \tag{2}$$

where x = z/z$_0$ and $q_0 = \frac{\sigma_{ex}\alpha F_0 L_{eff}}{2h\gamma}$. Here F_0 is the fluence of the laser at the focus and $L_{eff} = \frac{(1-\exp^{-\alpha L})}{\alpha}$.

The values of σ_{ex} of PThOxad 1a-c obtained through a fit of equation (2) to the corresponding open aperture data at 532 nm with q_0, are tabulated in Table 1. The value of ground state absorption cross-section of the polymers, as calculated from $\alpha = \sigma_g N_a C$, where N_a is Avogadro's number and C is the concentration in moles/cm^3, is also given in Table 1. It is clear that the value of σ_{ex} is larger than the value of σ_g in all the polymers, which is in agreement with the condition for observing the reverse saturable absorption (Henari et al., 1997; Tutt & Boggess, 1993). Reverse saturable absorption generally arises in a molecular system when the excited state absorption cross section is larger than the ground state cross section. The background linear absorption at 532 nm and the measured σ_{ex} values indicate that there is a contribution from excited state absorption to the observed NLA. This suggests that, the nonlinear absorption observed in the polymers can be attributed to a reverse saturable absorption.

Polymer	α (cm^{-1})	σ_g (x10^{-18} cm^2)	σ_{ex} (x10^{-17} cm^2)
PThOxad 1a	0.0487	8.092	9.66
PThOxad 1b	0.0622	10.32	5.44
PThOxad 1c	0.068	11.26	5.93

Table 1. The values of α, σ_g and σ_{ex} for the copolymers.

The reverse saturable absorption in these polymers can further be verified by plotting the nonlinear absorption coefficient against the incident intensity. Fig. 15 shows the plot of β versus the input intensity for PThOxad 1a-c in DMF at a concentration of 1x10^{-5} mol/L. Generally, nonlinear absorption (NLA) can be caused by free carrier absorption, saturated absorption, direct multiphoton absorption or excited state absorption. If the mechanism belongs to the simple two-photon absorption, β should be a constant that is independent of the on-axis irradiance I_0. If the mechanism is direct three-photon absorption β should be a linear increasing function of I_0 and the intercepts on the vertical axis should be nonzero (Guo et al., 2003). As shown in fig. 15, β is found to decrease with increasing input intensity. Such fall-off of β with increasing intensity is a consequence of the reverse

saturable absorption (Couris et al., 1995). With increasing intensity the total absorption of these polymers approaches asymptotically the absorbance of the triplet state. Therefore, the β will be reduced at least up to intensities where no other intensity dependence processes are involved which can further cause reduction of transmission of polymer solution.

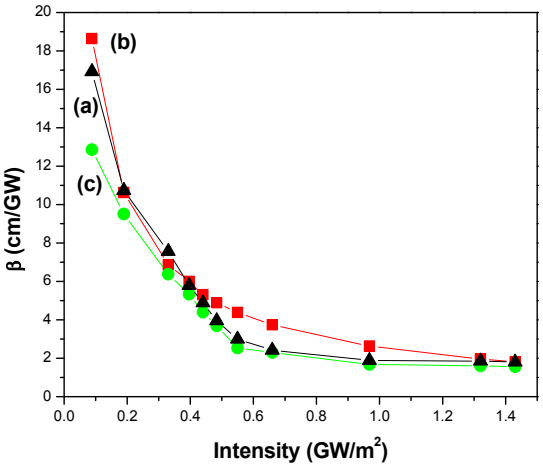

Fig. 15. β versus intensity for PThOxad 1a-c in DMF solution (1x10^{-5}mol/L). The magnitude of β decreased as intensity increased.

Fig. 16 shows the normalized transmission for the closed aperture Z-scan obtained for PThOxad 1a-c. These pure nonlinear refraction curves were obtained through dividing the closed aperture data by the corresponding open aperture data. The z-scan signature shows a large negative refractive nonlinearity (self defocusing) for all the polymers. The closed aperture data was fitted with equation (3) given below (Bahae et al., 1990; Liu et al., 2001):

$$T(z) = 1 - \frac{4\Delta\phi_0 x}{(1+x^2)(9+x^2)}, \tag{3}$$

where $\Delta\phi_o$ is the phase change given by $\Delta\phi_o = \frac{\Delta T_{p\text{-}v}}{0.406(1\text{-}S)^{0.25}}$ for $|\Delta\phi_o| \leq \pi$.

The values of nonlinear refractive index (n_2) for PThOxad1a-c were found to be of the order of 10^{-10} esu, and they are nearly two orders larger than the n_2 values reported for thiophene oligomers (Hein, 1994). The $\chi^{(3)}$ values of PThOxad 1a-c are comparable with 5x10^{-12} esu, reported for poly(3-dodecyloxymethylthiophene) (PDTh) (Bredas & Chance, 1989). The values of n_2 and $\chi^{(3)}$ estimated for the polymers PThOxad 1a-c are summarized in Table 2. These values were found to be consistent in all the trials with a maximum error of <10%.

Based on the strong reverse saturable absorption observed for PThOxad 1a-c, good optical limiting action can be expected from these polymers. In general, optical limiters have been utilized in a variety of circumstances where a decreasing transmission with increasing excitation is desirable. However, one of the most important applications is eye and sensor protection in optical systems (Tutt & Boggess, 1993). Fig. 17 demonstrates the optical

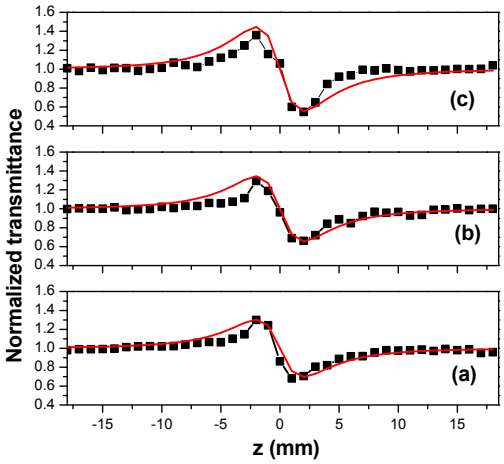

Fig. 16. Pure nonlinear refraction curve obtained for PThOxad 1a (a), PThOxad 1b (b) and PThOxad 1c (c). Solid lines are fit of data to equation (3) with $\Delta\Phi_0 = 1.5$ for PThOxad 1a, $\Delta\Phi_0 = 1.7$ for PThOxad 1b and $\Delta\Phi_0 = 2.2$ for PThOxad 1c.

Polymer	n_o	Z – scan n_2 (x10^{-10} esu)	Z – scan β (cm/GW)	DFWM Re $\chi^{(3)}$ (x10^{-12} esu)	DFWM Im $\chi^{(3)}$ (x10^{-12} esu)	DFWM $\chi^{(3)}$ (x10^{-12} esu)	DFWM F (x10^{-11} esu.cm)
PThOxad 1a	1.422	-1.942	73.8	-2.086	1.139	2.055	4.21
PThOxad 1b	1.422	-2.20	53.0	-2.366	0.818	2.39	3.84
PThOxad 1c	1.415	-2.836	63.6	-3.01	0.968	2.895	4.26

Table 2. Determined values of linear and nonlinear optical parameters for polymers under study.

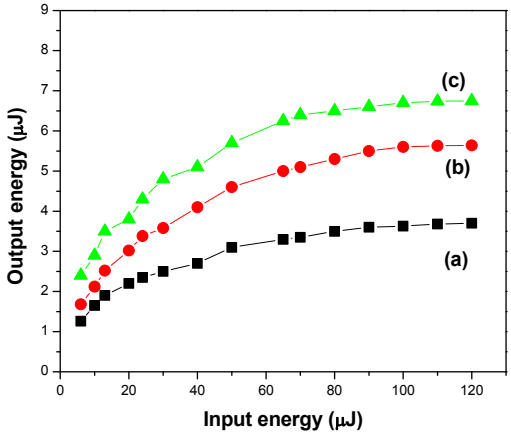

Fig. 17. Optical limiting behavior of PThOxad1a (a), PThOxad1b (b) and PThOxad1c (c), dissolved in DMF solution (1x10^{-5}mol/L).

limiting behavior of PThOxad 1a-c. The optical limiting was recorded by using the open aperture z-scan set up; the output energy transmitted by the sample was measured while the sample was kept fixed at the focus of the lens and the input energy was varied. For incident pule energies up to 20 μJ, the output was linearly increasing with the input. However, for energies more than around 20 μJ, optical limiting of pulses was observed in all the polymers. Although both nonlinear absorption and scattering can contribute to the optical limiting, no significant scattering from the samples was observed during the experiment within the energy limit used.

Concentration dependence of NLO properties can be analyzed to extract information on the NLO properties of the solute. The concentration of polymer in DMF solution was varied and the z-scan experiments were repeated on solutions at each concentration to study the variation of nonlinear response. Fig. 18 shows the dependence of nonlinear absorption (β) on the concentration of PThOxad 1a-c in solution. From $1x10^{-5}$ to $0.25x10^{-5}$ mol/L, β decreased linearly with the concentration, however, it was found to decrease rapidly below $0.25x10^{-5}$ mol/L. The nonlinear absorption as well as the nonlinear refraction decreased as the concentration of polymers in the solution decreased from $1x10^{-5}$ mol/L to $1.25x10^{-6}$ mol/L. Similarly the optical limiting behavior of the polymers was found to be dependent on the concentration. The optical limiting behaviors of PThOxad 1a-c were studied at different concentrations (E.g., fig. 19). Both the limiting threshold as well as the clamping level was found to vary the concentration. While the clamping level was found to be increasing with decreasing concentration, the optical limiting threshold was found to be increasing with decreasing concentration of the polymer in the DMF solution.

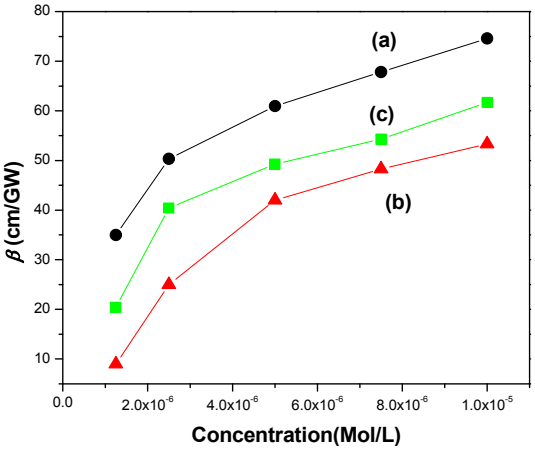

Fig. 18. Concentration dependence of β for polymers PThOxad 1a (a), PThOxad 1b (b) and PThOxad 1c (c).

The third-order NLO properties of two more series of polymers, PThOxad 2a-c and PThOxad 3a-c were also studied using the z-scan technique. The z-scan experiments were performed at pulse energy of 20 μJ which corresponds to a peak irradiance of 0.44 GW/cm^2. The sign of the nonlinear refractive index of these copolymers was also found to be negative

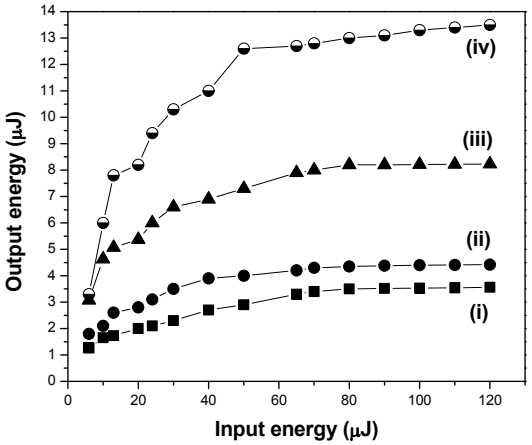

Fig. 19. Optical limiting behaviors of PThOxad 1a-c at different concentrations: (i) 1x10^{-5} Mol/L; (ii) 0.5xX10^{-5} Mol/L; (iii) 0.25x10^{-5} Mol/L: (iv) 0.125x10^{-5} Mol/L.

at 532 nm. The values of n_2 were –1.290x10^{-10}, –1.220x10^{-10} and –1.354x10^{-10} esu for PThOxad 2a-c, respectively. For PThOxad 3a-c, the values of n_2 were –1.121x10^{-10}, -1.212 x10^{-10} and -1.621 x10^{-10} esu, respectively. All the polymers exhibited strong reverse saturable absorption and very good optical limiting properties at 532 nm. The values of two-photon absorption coefficient (β) were 26, 24 and 32 cm/GW for PThOxad 2a-c, respectively. The corresponding values for PThOxad 3a-c were 20, 24 and 36 cm/GW, respectively. The magnitude of the $\chi^{(3)}$ was found to be of the order of 10^{-12} esu for all the polymers. The $\chi^{(3)}$ values were –1.38x10^{-12}, –1.315x10^{-12} esu for PThOxad 2a-c, respectively. For PThOxad 3a-c the corresponding values were –1.08x10^{-12}, –1.186x10^{-12} and -1.564 x10^{-12} esu, respectively.

Variation of the DFWM signal as a function of the pump intensity PThOxad 1c is shown in Fig. 20. The intensity dependence of the amplitude of the DFWM signal in other polymers was found to follow the similar pattern shown in the figure. The signal strength was proportional to the cubic power of the input intensity as given by the equation,

$$\mathrm{I}(\omega)\alpha\left(\frac{\omega}{2\varepsilon_0 cn^2}\right)^2\left|\chi^{(3)}\right|^2 l^2\,\mathrm{I}_0^3(\omega), \tag{4}$$

where $I(\omega)$ is the DFWM signal intensity, $I_0(\omega)$ is the pump intensity, l is the optical pathlength, and n is the refractive index of the medium. $\chi^{(3)}$ can be calculated from the equation:

$$\chi^{(3)} = \chi^{(3)}_{ref}\left[\frac{I/I_0^3}{(I/I_0^3)_{ref}}\right]^{1/2}\left[\frac{n}{n_{ref}}\right]^2\frac{l_{ref}}{l}\left(\frac{\alpha l}{(1-e^{-\alpha l})e^{-\frac{\alpha l}{2}}}\right), \tag{5}$$

where the subscript 'ref' refers to the standard reference CS_2 under identical conditions, and $\chi^{(3)}_{ref}$ is taken to be 4.0X10^{-13} esu (Philip et al., 1999; Shrik et al., 1992). The figure of merit F

was calculated using the equation $\chi^{(3)}/\alpha$. F is a measure of the nonlinear response that can be achieved for a given absorption loss, and is useful in comparing nonlinear materials in the region of absorption. The value of F is given in Table 2, which shows that the polymers possess good F values. It can be noted that the largest $\chi^{(3)}$ and F values have been measured for the polymer attached with highest electron donor among the copolymers. The value of $\chi^{(3)}$ measured by DFWM technique very well matches with the value of $\chi^{(3)}$ obtained by z-scan technique.

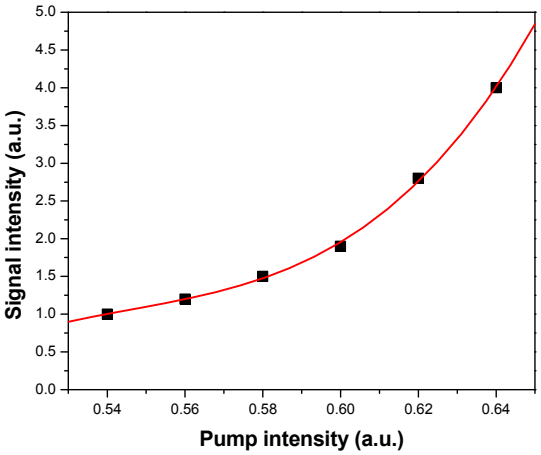

Fig. 20. Variation of the phase conjugate signal with the pump intensity PThOxad 1c. The solid line is a cubic fit of data.

4.2 Structure – NLO property relationship

Polymers PThOxad 1a-c contain alternating electron donating and electron withdrawing groups in their chain. The lengths of the alkoxy groups (-OR) at 3- and 4- positions of the thiophene rings play an important role in the third-order nonlinear response of the polymers. The alkoxy groups present in polymers PThOxad 1a-c are hexyloxy ($-OC_6H_{13}$), octyloxy ($-OC_8H_{17}$) and decyloxy ($-OC_{10}H_{21}$) respectively. The $\chi^{(3)}$ values of the polymers are found to be increasing from PThOxad 1a to PThOxad 1c. This can be attributed to the increase in the electron donating abilities of the alkoxy groups with increase in chain length. That is, the electron donating ability of alkoxy groups is in the order $-OC_6H_{13} < -OC_8H_{17} < -OC_{10}H_{21}$. Hence polymer PThOxad 1c, containing the longest alkoxy groups ($-OC_{10}H_{21}$) at 3- and 4- positions of the thiophene ring, shows the highest nonlinear response among the polymers. Therefore, the enhancement in third-order nonlinear response is attributed to the increased π-electron delocalization in the polymers. A similar variation has been observed in the nonlinear responses of polymers, PThOxad 2a-c. The observed nonlinear response of the polymers are in the order PThOxad 2a < PThOxad 2b < PThOxad 2c. Among three series of polymers (PThOxad 1a-c, PThOxad 2a-c and PThOxad 3a-c), polymers of PThOxad 1 series showed higher values of n_2 and $\chi^{(3)}$. The high nonlinear response of these polymers can be attributed to an increase in the effective conjugation length of the repeating unit due to the

presence of vinylene double bonds of 1,4-divinylbenzene unit in the main chain. Compared with PThOxad 3a-c, polymers PThOxad 2a-c show higher nonlinear response due to the presence of stronger electron donating 3,4-ethylenedioxythiophene units. These results suggest that the nonlinear optical properties of the polymers can be tuned by the structural design which involves introduction of alternating donor and acceptor groups along the polymer chain.

4.3 Polymer/TiO_2 nanocomposites

The open aperture z-scan curves obtained for the polymer (PThOxad 3c) film and the PThOxad 3c/TiO_2 composite films are shown in figs. 21 and 22 respectively. All the films show a strong optical limiting behavior. The effect is quite strong because the normalized transmission gets decreased to values like 0.1. In polymer composite systems under resonant excitation conditions, an optical limiting behavior can be attributed to effects such as excited state absorption (excited singlet and/or triplet absorption), two- or three-photon absorption (2PA, 3PA), self-focusing/defocusing, thermal blooming, and induced thermal scattering. Of these, 2PA, 3PA, and self focusing/defocusing are electronic nonlinearities that require high laser intensities usually available only from pulsed picosecond or femtosecond lasers. In the present case the possibilities are therefore that of excited state absorption, thermal blooming and induced thermal scattering. We did not visually observe any induced scattering, and the numerical aperture of the detector was large enough to accommodate the transmitted beam fully even if moderate thermal blooming were to happen. Therefore the cause of the observed optical limiting turns out to be excited state absorption. It is possible to model excited state absorption as an "effective" 2PA or 3PA for numerical convenience, and when we tried to fit the experimental data to standard nonlinear transmission equations accordingly, the existence of a relatively weaker saturable absorption also came to light. Therefore an effective intensity-dependent nonlinear absorption coefficient of the form,

$$\alpha(I) = \frac{\alpha_0}{1 + (I / I_s)} + \beta I \tag{6}$$

can be considered, where α_0 is the unsaturated linear absorption coefficient at the wavelength of excitation, I is the input laser intensity, and I_s is the saturation intensity (intensity at which the linear absorption drops to half its original value). $\beta I = \sigma N$ is the excited state absorption (ESA) coefficient, where σ is the ESA cross section and N(I) is the intensity-dependent excited state population density. For calculating the transmitted intensity for a given input intensity, the propagation equation,

$$\frac{dI}{dz'} = -\left[\left(\alpha_0 \Big/ \left(1 + \frac{I}{I_s}\right)\right) + \beta I\right] I \tag{7}$$

was numerically solved. Here z' indicates the propagation distance within the sample. By determining the best-fit curves for the experimental data, the nonlinear parameters could be calculated.

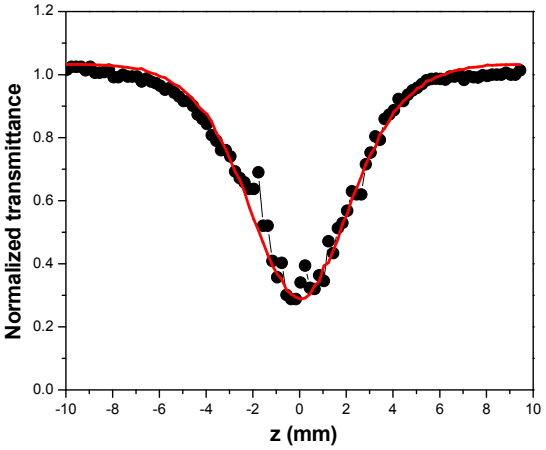

Fig. 21. Open aperture z-scan of polymer film having a linear transmission of 59 % at 532 nm. The laser pulse energy is 90 microJoules. Circles are data points while the solid curve is a numerical fit according to equation (6).

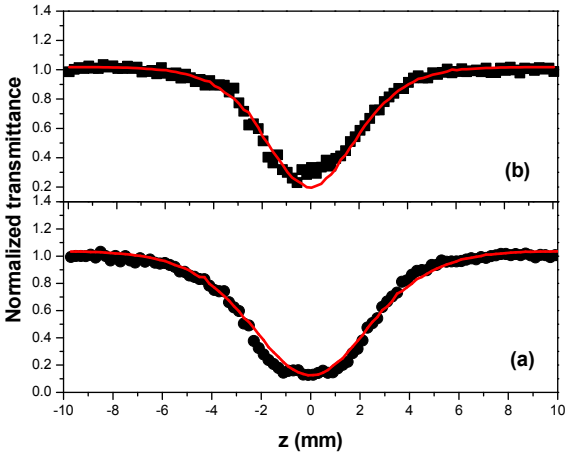

Fig. 22. Open aperture z-scan of nanocomposite films having a linear transmission of 51% at 532 nm. The laser pulse energy is a) 100 microJoules, b) 75 microJoules. Circles are data points while the solid curve is a numerical fit according to equation (6).

For PThOxad 3c film, β is found to be 1 x 10^{-7} m/W, while for the nanocomposite film it is 2 x 10^{-7} m/W. Obviously there is an enhancement of nonlinearity in PThOxad 3c/TiO_2

nanocomposite film compared to the pure PThOxad 3c film. This is not substantial though, the reason being that the polymer films themselves are highly nonlinear in nature. From a device point of view both PThOxad 3c and PThOxad 3c/TiO_2 nanocomposite films are equally useful because the optical limiting efficiency exhibited by them is high. To put the above β values in perspective, the values obtained in similar systems under similar excitation conditions are, 6.0 x 10^{-8} m/W in p-(N,N-dimethylamino)dibenzylideneacetone in PMMA matrix (Kiran et al., 2008), 10^{-7} to 10^{-9} m/W in Au:Ag-PVA nanocomposite films and 6.8 x 10^{-7} m/W in a ZnO/PMMA nanocomposite (Sreeja et al., 2010). Obviously, the present films are potentially suited for fabricating optical limiters, which can protect sensitive light detectors and also human/animal eyes from accidental exposure to high levels of optical radiation, while maintaining normal transparency for safe low level inputs.

5. Conclusions

The third-order nonlinear optical properties of three series of Donor-Acceptor polymers containing oxadiazole and substituted thiophene units and of a polymer/TiO_2 nanocomposite film have been investigated by using z-scan and DFWM techniques in the nanosecond domain. The results indicated that a nonlinear refractive index of the order of 10^{-10} esu can be readily obtained in these D-A polymers. The magnitude of $\chi^{(3)}$ is found to be of the order of 10^{-12} esu for all the polymers. The nonlinear absorption is found to be originating from the reverse saturable absorption. The polymers exhibit good optical limiting properties at 532 nm. The results showed that the polymer PThOxad 1c, containing the longest alkoxy group, exhibits highest nonlinearity among the three series of polymers and it may be a potential candidate for optical limiting, optical switching and other fast photonic applications. The dependence of NLO parameters on the length of the alkoxy substituents present in the polymers indicates that the nonlinearity in these polymers originates from the electronic effects. The nonlinear absorption, nonlinear refraction and optical limiting behavior of the polymers increase with increasing sample concentration in solution. In PThOxad 3c/TiO_2 nanocomposite, incorporation of TiO_2 nanoparticles into the polymer matrix is found to improve the thermal stability of the polymer. A red shift in the absorption spectra and a blue shift in the emission spectra are observed for PThOxad 3c/TiO_2 nanocomposite film compared to those of PThOxad 3c film. The composite film showed a strong optical limiting behavior, and the incorporation of TiO_2 marginally enhanced the nonlinear absorption coefficient value of the polymer. The present study reveals that the third-order nonlinear optical properties of conjugated polymers can be enhanced by increasing the π-electron delocalization along the polymer chain through a proper structural modification. Further, the results show that the nonlinear effects in a conjugated polymer can be enhanced by incorporating TiO_2 nanoparticles in to the polymer matrix.

6. Acknowledgements

We thank Dr. Reji Philip, Raman Research Centre Bangalore, India for useful suggestions and for providing facility for the NLO experiments.

7. References

Boyd, R.W.; Gehr, R.J.; Fischer, G.L. & Sipe, J.E. (1996). Nonlinear Optical Properties of Nanocomposite Materials. *Pure and Applied Optics*, Vol.5, No.5, (September 1996), pp. 505-512, ISSN 1361-6617.

Bredas, J.L. & Chance, R.R. (1989). *Conjugated Polymeric Materials Opportunities in Electronics, Optoelectronics and Molecular Electronics,* ISBN 13-9780792307518, Kluwer Academic publishers, USA.

Brocks, G. & Tol, J. (1996). Small Band Gap Semiconducting Polymers Made from Dye Molecules: Polysquaraines. *Journal of Physical Chemistry*, Vol.100, No.5, (February 1996), pp. 1838-1848, ISSN 1520-5207.

Cassano, T.; Tommasi, R.; Babudri, F.; Cardone, A.; Farinola, G.M. & Naso, F. (2002). High Third-Order Nonlinear Optical Susceptibility in New Fluorinated Poly(p-phenylenevinylene) Copolymers Measured with the Z-scan Technique. *Optical Letters*, Vol.27, No.24, (December 2002), pp. 2176-2178, ISSN 1539-4794.

Chen, Q.; Sargent, E.H.; Leclerc, N. & Attias, A.J. (2003). Wavelength Dependence and Figures of Merit of Ultrafast Third-Order Optical Nonlinearity of a Conjugated 3,3′-Bipyridine Derivative. *Applied Optics*, Vol.42, No.36, (December 2003), pp. 7235-7241, ISSN 2155-3165.

Chen, X.; Tao, J.; Zou, G.; Zhang, Q. & Wang, P. (2010). Nonlinear Optical Properties of Nanometer-Size Silver Composite Azobenzene Containing Polydiacetylene Film. *Applied Physics A*, Vol.100, No.1, (February 2010), pp. 223-230, ISSN 1432-0630.

Couris, S.; Koudoumas, E.; Ruth, A.A. & Leach, S. (1995). Concentration and Wavelength Dependence of the Effective Third-Order Susceptibility and Optical Limiting of C_{60} in Toluene Solution. *Journal of Physics B: Atomic, Molecular and Optical Physics,* Vol.28, No.20, (October 1995), pp. 4537-4554, ISSN 1361-6455.

Davey, A.P.; Elliott, S.; Connor, O.O. & Blau, W. (1995). New Rigid Backbone Conjugated Organic Polymers with Large Fluorescence Quantum Yields. *Journal of the Chemical Society, Chemical Communications*, No.14, pp. 1433-1434, (January 1995), ISSN 0022-4936.

Demas, J.N. & Crosby, G.A. (1971). Measurement of Photoluminescence Quantum Yields. *Journal of Physical Chemistry*, Vol.75, No.8, (April 1971), pp. 991-1024, ISSN 1932-7447.

Fatti, N.D. & Vallee, F. (2001). Ultrafast Optical Nonlinear Properties of Metal Nanoparticles. *Applied Physics B*, Vol.73, No.4, (October 2001), pp. 383-390, ISSN 1432-0649.

Gao, Y.; Tonizzo, A.; Walser, A.; Potasek, M. & Dorsinville, R. (2008). Enhanced Optical Nonlinearity of Surfactant-Capped CdS Quantum Dots Embedded in an Optically Transparent Polystyrene Thin Film. *Applied Physics Letters,* Vol.92, No.3, (January 2008), pp. 033106-033109, ISSN 1077-3118.

Gayvoronsky, V.; Galas, A.; Shepelyavyy, E.; Dittrich, Th.; Timoshenko, V.Yu.; Nepijko, S.A.; Brodyn, M.S. & Koch, F. (2005). Giant Nonlinear Optical Response of Nanoporous Anatase Layers. *Applied Physics B*, Vol.80, No.1, (November 2005), pp. 97-100, ISSN 1432-0649.

Guo, S.Li.; Xu, L.; Wang, H.T.; You, X.Z. & Ming, N.B. (2003). Investigation of Optical Nonlinearities in $Pd(po)_2$ by Z-scan Technique. *Optik - International Journal for Light and Electron Optics*, Vol.114, No.2, (November 2003), pp. 58-62, ISSN 0030-4026.

Havinga, E.E.; Hoeve, W. & Wynberg, H. (1993). Alternate Donor-Acceptor Small Band Gap Semiconducting Polymers; Polysquaraines and Polycroconaines. *Synthetic Metals*, Vol.55, No.1, (March 1993), pp. 299-306, ISSN 03796779.

Hegde,; P.K. Vasudeva Adhikari,; A. Manjunatha, M.G.; Suchand Sandeep, C.S. & Reji Philip (2009). Synthesis and Nonlinear Optical characterization of New poly*{*2,2'-(3,4-didodecyloxythiophene-2,5-diyl)bis[5-(2-thienyl)-1,3,4-oxadiazole]*}*. *Synthetic Metals*, Vol.159, No.11, (June 2009), pp. 1099–1105, ISSN 0379-6779.

Hein, J.; Bergner, H.; Lenzner, M. & Rentsch, S. (1994). Determination of Real and Imaginary Part of $\chi^{(3)}$ of Thiophene Oligomers using the Z-scan Technique. *Chemical Physics*, Vol.179, No.3, (February 1994), pp. 543-548, ISSN 0301-0104.

Henari, F.Z.; Blau, W.J.; Milgrom, L.R.; Yahioglu, G.; Philips, D. & Lacey, J.A. (1997). Third-Order Optical Non-Linearity in Zn(II) Complexes of 5,10,15,20-tetraarylethynyl-Substituted Porphyrins. *Chemical Physics Letters*, Vol.267, No.3-4, (March 1997), pp. 229-233, ISSN 0009-2614.

Hsieh, S.N.; Wen, T.C. & Guo, T.F. (2007). Polymer/Gold Nanoparticles Light Emitting Diodes Utilizing High Work Function Metal Cathodes. *Materials Chemistry and Physics*, Vol.101, No.2-3, (February 2007), pp. 383-386, ISSN 0254-0584.

Hu X.Y.; Jiang, P.; Ding, C.Y.; Yang, H. & Gong, Q.H. (2008). Picosecond and Low-Power all-Optical Switching based on an Organic Photonic-Bandgap Microcavity. *Nature Photonics*, Vol.2, No.3, (March 2008), pp. 185-189, ISSN 1749-4885.

Hu, X.; Zhang, J.; Yang, H. & Gong, Q. (2009). Tunable Time Response of the Nonlinearity of Nanocomposites by Doping Semiconductor Quantum Dots. *Optics Express*, Vol.17, No. 21, (October 2009), PP. 18858-18865, ISSN 1094-4087.

Kamanina, N.V. & Plekhanov, A.I. (2002). Mechanisms of Optical Limiting in Fullerene-Doped π-Conjugated Organic Structures Demonstrated with Polyimide and COANP Molecules. *Optics and Spectroscopy*, Vol.93, No.3, (September 2002), pp. 408-415, ISSN 1562-6911.

Kamanina, N.V. (1999). Reverse Saturable Absorption in Fullerene-Containing Polyimides, Applicability of the Förster Model. *Optical Communication*, Vol.162, No.4-6, (April 1999), pp. 228–232, ISSN 0030-4018.

Kamanina, N.V. (2001). Peculiarities of Optical Limiting Effect in π-Conjugated Organic Systems based on 2-cyclooctylamino-5-nitropyridinedoped with C_{70}. *Journal of Optics A Pure and Applied Optics*, Vol.3, No.5, (July 2001), pp. 321-325, ISSN 1464-4258.

Kamanina, N.V.; Reshak, A.H.; Vasilyev, P.Ya.; Vangonen, A.I.; Studeonov, V.I.; Usanov, Yu.E.; Ebothe, J.; Gondek, E.; Wojcik, W. & Danel, A. (2009). Nonlinear Absorption of Fullerene and Nanotubes Doped Liquid Crystal Systems. *Physica E*, Vol.41, No.3, (January 2009), pp. 391-394, ISSN 13869477.

Kamanina, N.V.; Vasilyev, P.Ya.; Vangonen, A.I.; Studeonov, V.I.; Usanov, Yu.E.; Kajzar, F. & Attias, A.J. (2008). Photophysics of Organic Structures Doped with Nanoobjects:

Optical Limiting, Switching and Laser Strength. *Moleculer Crystals and Liquid crystals*, Vol.485, No.1, (April 2008), pp. 945-954, ISSN 1563-5287.

Karthikeyan, B.; Anija, M. & Reji Philip, (2006). In Situ Synthesis and Nonlinear Optical Properties of Au:Ag Nanocomposite Polymer films. Applied Physics Letters, Vol.88, No.5, (January 2006), pp. 053104-053107, ISSN 1077-3118.

Kiran, A.J.; Rai, N.S.; Udayakumar, D.; Chandrasekharan, K.; Kalluraya, B.; Reji Philip, Shashikala, H.D. & Adhikari, A.V. (2008). Nonlinear Optical properties of p-(N,N-dimethylamino) dibenzylidene -acetone Doped Polymer. *Material Research Bulletin*, Vol.43, No.3-4, (March 2008), pp. 707-713, ISSN 0025-5408.

Kiran, A.J.; Udayakumar, D.; Chandrasekharan, K.; Adhikari, A.V. & Shashikala, H.D. (2006). Z-scan and Degenerate Four Wave Mixing Studies on Newly Synthesized Copolymers Containing Alternating Substituted Thiophene and 1,3,4-oxadiazole units. *Journal of physics B: Atomic molecular and optical physics*, Vol.39. No.18, (September 2006), pp. 3747–3756, ISSN 0953-4075

Kishino, S.; Ueno, Y.; Ochiai, K.; Rikukawa, M.; Sanui, K.; Kobayashi, T.; Kunugita, H.; & Ema, K. (1998). Estimate of the effective conjugation length of polythiophene from its $|\chi^{(3)}(\omega;\omega,\omega,-\omega)|$ spectrum at excitonic resonance. *Physical Review B*, Vol. 58, No. 20, PP. R13430-R13433, (November 1998) ISSN 1943-2879.

Liu, X.; Guo, S.; Wang, H. & Hou, L. (2001). Theoretical Study on the Closed-Aperture Z-scan Curves in the Materials with Nonlinear Refraction and Strong Nonlinear Absorption. *Optics Communications*, Vol.197, No.4-6, (October 2001), pp. 431-437, ISSN 0030-4018.

Munn, R.W. & Ironside, C.N. (1993). *Principles and Applications of Nonlinear Optical Materials*, ISBN 10-0751400858, Routledge Chapman Hall.

Neeves, A.E. & Birnboim, M.H. (1988). Composite Structures for the Enhancement of Nonlinear Optical Materials. *Optics Letters*, Vol.13, No.12, (December 1988), pp. 1087-1089, ISSN 1539-4794.

Nisoli, M.; Cybo-Ottone, A.; De Silvestri, S.; Magni, V.; Tubino, R.; Botta, C. & Musco, A. (1993). Femtosecond Transient Absorption Saturation in Poly(alkyl-thiophene-vinylene)s. *Physical Review B*, Vol.47, No.16, (April 1993), pp. 10881-10884, ISSN 1943-2879.

Philip, R.; Ravikanth, M. & Ravindrakumar, G. (1999). Studies of Third Order Optical Nonlinearity in Iron (III) Phthalocyanine μ-oxo Dimers Using Picosecond Four-wave Mixing. *Optics Communications*, Vol.165, No.1-3, (July 1999), pp. 91-97, ISSN 0030-4018.

Porel, S.; Venkataram, N.; Rao, D.N. & Radhakrishnan, T.P. (2007). Optical Power Limiting in the Femtosecond Regime by Silver Nanoparticle–Embedded Polymer Film. *Journal Applied Physics*, Vol.102, No.3, (August 2007), pp. 033107-033113, ISSN 1077-3118.

Prasad, P.N. & Williams, D.J. (1992). *Introduction to Nonlinear Optical Effects in Molecules and Polymers*, ISBN 978-0-471-51562-3, John Wiley & Sons, New York.

Reji Philip; Ravindrakumar, G.; Sandhyarani, N. & Pradeep, T. (2000). Picosecond Optical Nonlinearity in Monolayer-Protected Gold, Silver, and Gold-Silver Alloy

Nanoclusters. *Physical Review B*, Vol.62, No.19, (November 2000), pp. 13160-13166, ISSN 1943-2879.

Sezer, A.; Gurudas, U.; Collins, B.; Mckinlay, A. & Bubb, D.M. (2009). Nonlinear Optical Properties of Conducting Polyaniline and Polyaniline–Ag Composite Thin Films. *Chemical Physics Letters*, Vol.477, No.1-3, (July 2009), ISSN 0009-2614.

Sheik Bahae, M.; Said, A.A.; Wei, T.H.; Hagan, D.J. & Stryland, E.W.Van. (1990). Sensitive Measurement of Optical Nonlinearities using a Single Beam. *IEEE Journal of Quantum Electronics,* Vol.26, No.4, (April 1990), pp. 760-769, ISSN 0018-9197.

Shrik, J.S.; Lindle, J.R.; Bartoli, F.J. & Boyle, M.E. (1992). Third-Order Optical Nonlinearities of bis(phthalocyanines). *Journal of Physical Chemistry*, Vol.96, No.14, (July 1992), pp. 5847-5852, ISSN 1932-7447.

Sreeja, R.; John, J.; Aneesh, P.M. & Jayaraj, M.K. (2010). Linear and Nonlinear Optical Properties of Luminescent ZnO Nanoparticles Embedded in PMMA Matrix. *Optics Communications*, Vol.283, No.14-15, (July 2010), pp. 2908-2913, ISSN 0030-4018.

Sutherland, R.L. (1996). *Hand Book of Nonlinear Optics*, ISBN 0-8247-9651-9, Marcel Dekker Inc., New York.

Takele, H.; Greve, H.; Pochstein, C.; Zaporojtchenko, V. & Faupel, F. (2006). Plasmonic Properties of Ag Nanoclusters in Various Polymer Matrices. *Nanotechnology*, Vol.17, No.14, (July 2006), pp. 3499-3504, ISSN 1361-6528.

Tutt, L.W. & Boggess T.F. (1993). A Review of Optical Limiting Mechanisms and Devices using Organics, Fullerenes, Semiconductors and other Materials. *Progress in Quantum Electronics*, Vol.17, No.4, (August 1993), pp. 299-338, ISSN 0079-6727.

Udayakumar, D.; John Kiran, A.; Adhikari, A.V.; Chandrasekharan, K. & Shashikala, H.D. (2007). Synthesis and Nonlinear Optical Characterization of Copolymers Containing Alternating 3,4-dialkoxythiophene and (1,3,4-oxadiazolyl)benzene units. *Journal of Applied Polymer Science*, Vol. 106, No.5, (December 2007), pp. 3033–3039, ISSN 1097-4628.

Udayakumar, D.; John Kiran, A.; Vasudeva Adhikari, A.; Chandrasekharan, K.; Umesh, G. & Shashikala H.D. (2006). Third-Order Nonlinear Optical Studies of Newly Synthesized polyoxadiazoles Containing 3,4-dialkoxythiophenes. *Chemical Physics*, Vol.331, No.1, (December 2006), pp. 125-130, ISSN 0301-0104.

Venkatram, N.; Rao, D.N. & Akundi, M.A. (2005). Nonlinear Absorption, Scattering and Optical Limiting Studies of CdS nanoparticles. *Optics Express*, Vol.13, No.3, (February 2005), PP. 867-872, ISSN 1094-4087.

Voisin, C. ; Del Fatti, N.; Christofilos, D. & Vall´ee F. (2001). Ultrafast Electron Dynamics and Optical Nonlinearities in Metal Nanoparticles. *Journal of Physical Chemistry B*, Vol.105, No.12, (March 2001), pp. 2264-2280, ISSN 1089-5647.

Yang, P.; Xu, J.; Ballato, J.; Schwartz, R.W. & Carroll, D.L. (2002). Optical Limiting in $SrBi_2Ta_2O_9$ and $PbZr_xTi_{1-x}O_3$ Ferroelectric Thin Films. *Applied Physics Letters,* Vol.80. No.18, (April 2002), pp. 3394-3397, ISSN 1077-3118.

Yang, S.H.; Rendu, P.L.; Nguyen, T.P. & Hsu, C.S. (2007). Fabrication of MEH-PPV/SiO_2 and MEH-PPV/TiO_2 Nanocomposites with Enhanced Luminescent Stabilities. *Reviews on Advanced Materials Science*, Vol.15, No.2,

Zhu, Y.; Xu, S.; Jiang, L.; Pan, K. & Dan, Y. (2008). Synthesis and Characterization of Polythiophene/Titanium dioxide Composites. *Reactive and Functional Polymers*, Vol.68, No.10, (October 2008), pp. 1492-1498, ISSN 1381-5148.

Zyss, J. (1994). *Molecular Nonlinear Optics, Materials, Physics and Devices*, ISBN 978-0-12-784450-3, Academic Press.

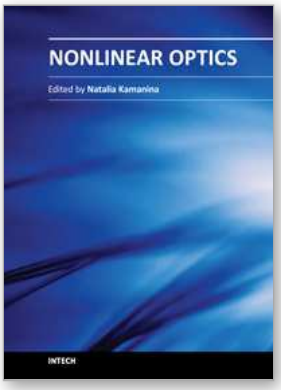

Nonlinear Optics

Edited by Dr. Natalia Kamanina

ISBN 978-953-51-0131-4
Hard cover, 224 pages
Publisher InTech
Published online 29, February, 2012
Published in print edition February, 2012

Rapid development of optoelectronic devices and laser techniques poses an important task of creating and studying, from one side, the structures capable of effectively converting, modulating, and recording optical data in a wide range of radiation energy densities and frequencies, from another side, the new schemes and approaches capable to activate and simulate the modern features. It is well known that nonlinear optical phenomena and nonlinear optical materials have the promising place to resolve these complicated technical tasks. The advanced idea, approach, and information described in this book will be fruitful for the readers to find a sustainable solution in a fundamental study and in the industry approach. The book can be useful for the students, post-graduate students, engineers, researchers and technical officers of optoelectronic universities and companies.

How to reference

In order to correctly reference this scholarly work, feel free to copy and paste the following:

D. Udaya Kumar, A. John Kiran, M. G. Murali and A. V. Adhikari (2012). Donor-Acceptor Conjugated Polymers and Their Nanocomposites for Photonic Applications, Nonlinear Optics, Dr. Natalia Kamanina (Ed.), ISBN: 978-953-51-0131-4, InTech, Available from: http://www.intechopen.com/books/nonlinear-optics/donor-acceptor-conjugated-polymers-and-their-nancomposites-for-photonic-applications

INTECH
open science | open minds

InTech Europe
University Campus STeP Ri
Slavka Krautzeka 83/A
51000 Rijeka, Croatia
Phone: +385 (51) 770 447
Fax: +385 (51) 686 166
www.intechopen.com

InTech China
Unit 405, Office Block, Hotel Equatorial Shanghai
No.65, Yan An Road (West), Shanghai, 200040, China
中国上海市延安西路65号上海国际贵都大饭店办公楼405单元
Phone: +86-21-62489820
Fax: +86-21-62489821